Peer review status:

This is a non-peer-reviewed preprint submitted to EarthArXiv.

It has been submitted for peer review to *Earth, Planets and Space* as an Express Letter.

Data: the table of 158 ruptures and the script that recomputes the scores are at `https://doi.org/10.5281/zenodo.23602567`.

License: CC BY 4.0.

The width beyond a static arrest point predicts which static arrests span the fault

Wenjie Lyu
School of Civil Engineering, China University of Mining and Technology, Xuzhou, China
WenjieLyu02@gmail.com
https://orcid.org/0009-0009-3039-7727

The width beyond a static arrest point predicts which static arrests span the fault

Wenjie Lyu (corresponding author), School of Civil Engineering, China University of Mining and Technology, Xuzhou, China, WenjieLyu02@gmail.com

Preprint submitted to *Earth, Planets and Space* on November 3, 2026

Abstract
Population models treat a static arrest as the end of the rupture, although some of those arrests span the fault in a fully dynamic calculation. This paper tests whether the static crack itself shows which ones. A static stress-intensity criterion and a fully dynamic rupture were compared on 180 new random stress fields on one 120 km antiplane fault with linear slip weakening. The predictor is the subcritical width, the extra distance one crack tip must be extended, with the other tip held fixed, before the static stress intensity factor returns to its critical value. Two logistic models were fitted on 52 earlier antiplane ruptures, 10 of which span the fault. One uses the static arrest length alone and the other adds the width. Both were applied unchanged to the 158 new ruptures that the static criterion stops. Of the 158, 24 span the fault dynamically. Adding the width raises the probability that a spanning rupture ranks above an arrested one from 0.880 to 0.956, a gain of 0.076 with a 95% interval from 0.037 to 0.126. The test and the required gain were fixed before the new fields were drawn. Halving the grid spacing along strike left the outcome of all 158 ruptures unchanged. On 120 earlier ruptures on the same fault, the static criterion and the dynamic rupture disagreed 22 times, and all 22 were static arrests that spanned the fault. Population models and induced earthquake estimates that use the static balance make that error in one direction. The width read from the static crack can rank which of those static arrests should be run dynamically first, at the correlation length tested here. At a correlation length 1.78 times longer, a width threshold flags 19 of 38 spanning ruptures and a length threshold flags 34, so that ranking is not shown to carry over. The test covers antiplane rupture, one correlation length, three stress amplitudes, and linear slip weakening.

Keywords
dynamic rupture, rupture arrest, slip weakening, subcritical width

1 Introduction

Population models stop each rupture with a static or semi-dynamic balance between energy release and fracture energy (Ampuero et al. 2006; McLaskey et al. 2026). The same balance is used to estimate how large an induced rupture can grow (Galis et al. 2017). A rupture is counted as arrested when the balance fails, and as spanning the fault when it does not. The static length is used in place of a dynamic calculation.

On the same fault, that use of the static length fails in one direction (Lyu 2026a). In 22 of 120 earlier ruptures the static rule predicted arrest and the fully dynamic rupture ran to the end of the fault. None of the disagreements ran the other way. A calculation that trusts the static length will therefore record some fault-spanning ruptures as stopped.

Which static arrests later span the fault is only partly shown by the length of the static crack. The quantity used here is the subcritical width. It is the extra distance one crack tip must be extended, with the other tip held fixed, before the static stress intensity factor returns to its critical value (Fig. 1). A short width means the static rule has stopped the rupture just before a region in which the same static calculation would let it grow again. Weng et al. (2015) placed a barrier of raised normal stress on an otherwise uniform in-plane fault. A barrier below a lower size allowed the rupture to pass at subshear speed, a barrier above an upper size stopped it, and intermediate sizes could start a supershear rupture. The width in this paper is measured after the static rule has stopped the crack, on the random initial stress (Fig. 2).

This paper reports a test on 180 new two-dimensional dynamic ruptures on one 120 km fault. The prediction, its coefficients, and the required gain were fixed before the stress fields were drawn. The width was selected on 52 earlier antiplane ruptures, so those ruptures cannot test it. On 158 new ruptures that the static rule stops, the width is added to the static arrest length. This raises the probability that a spanning rupture ranks above an arrested one by 0.076, with a 95% interval from 0.037 to 0.126 (Fig. 3). None of the 158 changes outcome when the spacing along strike is halved. The result changes which static arrests a population model should check dynamically first, at this correlation length: on the ruptures tested, the width ranks them better than the static length alone. In laboratory experiments, static triggering and a barrier-induced supershear transition can carry a rupture past a barrier that linear-elastic fracture mechanics expects to stop (Paglialunga et al. 2026). On a slip-weakening fault, a rupture can also jump from a sub-Rayleigh speed to an intersonic speed by opening a daughter crack ahead of the front. On a uniform fault that transition requires the strength ratio to lie below a critical value (Dunham 2007). The same separation on new in-plane ruptures remains open. The earlier 52 in-plane ruptures gave a gain of 0.036 whose interval included zero (Lyu 2026a).

2 Methods

2.1 Fault and initial stress

The comparison below was fixed before the new stress fields were drawn. The fault, friction, and random stress are those of Lyu (2026a). The fault is 120 km long in a uniform elastic full space. Friction is linear slip weakening (Ida 1972; Andrews 1976) with a slip-weakening distance $D_c = 0.4$ m. The initial shear stress is a zero-mean normal random field with the spectrum of Ampuero et al. (2006), Hurst exponent 1, and a correlation length of 2.03 km. Their Figure 1 uses a correlation length of five antiplane nucleation half-lengths, and the half-length is the critical nucleation size of Uenishi and Rice (2003). The standard deviation of the initial stress is 0.343, 0.393, or 0.443 times the strength drop, with 60 fields at each value. The hypocenter is at least 40 km from either end of the fault. The random seed, 20261101, had not been used before.

2.2 Static arrest length and subcritical width

The static arrest length comes from the rule of Ampuero et al. (2006). That rule uses the static stress intensity factor after initiation. Campillo and Ionescu (1997) analyzed the earlier stage, in which antiplane slip on a slip-weakening fault grows exponentially in time. Starting from the nucleation patch, each crack tip advances in steps of 0.1 km while its static stress intensity factor exceeds the critical value K_c, and stops otherwise. A static crack at least 108 km long is counted as spanning the fault. Of the 180 fields, 22 reach that length and are not in the test. On four of the remaining ruptures one tip already lies on an end of the fault, so that side has no width beyond the tip. The predictor then uses the other side. All four span the fault in the dynamic calculation. Additional file 1 leaves those four entries blank.
On each side that still has fault ahead of the tip, the subcritical width is the further extension of that tip, with the other tip held fixed, at which the static stress intensity factor again reaches K_c. The extension uses steps of 0.1 km. If the next step would leave the fault, the width is the last step that remains on the fault, and that side is marked as cut off. The predictor is the larger of the recorded side widths, divided by $\Lambda = \mu D_c/(\tau_p - \tau_d) = 0.703$ km. Palmer and Rice (1973) estimated the length of the end zone on a slip surface, the interval in which shear stress falls from its peak value to its residual value. The cohesive zone of a propagating rupture was not measured on these ruptures. The static arrest length and the side widths were recorded before any dynamic rupture was run. Figure 1 defines that measurement. Figure 2 shows it on two of the 158 ruptures: one near the median width among those that span the fault, and one near the median width among those that stop in both calculations.

2.3 Dynamic ruptures

The dynamic ruptures are antiplane and are solved with `fdfault` (Daub 2017) with 200 m spacing along strike. A dynamic rupture is counted as spanning the fault when the nodes whose final slip reaches D_c cover at least 108 km. Every rupture that the static criterion stops was rerun with 100 m spacing along strike.

2.4 Unchanged prediction and test

Two logistic regression models were fitted to the 52 earlier antiplane ruptures, 10 of which span the fault dynamically. The predictors are the natural logarithm of the static arrest length in kilometers and the natural logarithm of the subcritical width divided by Λ. On those 52 ruptures the means of the two logarithms are 3.0506 and 2.8694. The square roots of the average squared deviations from those means, dividing by 52, are 0.7267 and 1.4658. Each new rupture is standardized with these four numbers before the coefficients are applied. The fit penalized the sum of the squared coefficients by 1 and did not penalize the intercept. The coefficients were recorded and applied unchanged to the 158 new ruptures. With z_L and z_w the standardized logarithms, the length-only score is $-1.8801 + 1.3114\, z_L$. The two-variable score is $-2.3679 + 1.3221\, z_L - 1.1496\, z_w$. The predicted probability of spanning the fault is $1/(1 + e^{-\text{score}})$. The area under the curve (AUC) is the probability that a randomly chosen rupture that spans the fault receives a higher predicted probability than a randomly chosen rupture that stops. The gain is the AUC of the second model minus that of the first, on the new ruptures. Its 95% interval comes from 2000 resamples of the new ruptures, drawn separately among those that span and those that stop, with both AUCs recomputed on each resample. Before the new fields were drawn, the gain was required to be at least 0.03, with the lower end of the interval above zero. At 100 m spacing the gain was required to stay positive, and fewer than 20% of the ruptures that spanned at 200 m were allowed to change outcome.

3 Results

3.1 Prediction on the new ruptures

On the new ruptures, the subcritical width separates static arrests that span the fault from static arrests that do not. Later sections test the grid spacing, the sides cut off at the fault end, and the distance from the arrest point to the fault end. Of the 180 new fields, the static criterion stops the rupture in 158. In 24 of the 158 the dynamic rupture spans the fault. The first model reached an AUC of 0.880 and the second 0.956. The gain is 0.076, with a 95% interval from 0.037 to 0.126. The median normalized subcritical width is 3.27 among the 24 and 29.3 among the other 134 (Fig. 3a). When the second model is refitted on the new ruptures, the width coefficient is -1.75. A shorter subcritical width corresponds to a higher probability of spanning the fault.

3.2 Grid spacing and resampling

The finer grid does not remove the separation. With 100 m spacing, none of the 24 stopped and none of the 134 spanned the fault. The gain computed with the 100 m outcomes is 0.076, with an interval from 0.036 to 0.127. At 200 m the static estimate Λ covers about 3.5 grid intervals. Day et al. (2005) found that their finite-difference solutions needed about five nodes inside the cohesive zone of a propagating rupture. The classification is unchanged on the finer grid. The numerical value of the width itself was not checked for convergence. Resampling within each stress amplitude and each outcome together gives an interval from 0.035 to 0.125 for the same gain. The interval from 0.036 to 0.127 resamples each outcome on its own.
Refitting within the new ruptures, and scoring each rupture with a model that did not use it, gives a gain of 0.079, with an interval from 0.030 to 0.141. The reported gain is the one from the coefficients fitted on the earlier 52.

3.3 Sides cut off at the fault end

Cutting a side off at the fault end could raise the gain even if the width itself did not. In 58 ruptures at least one side is cut off by the fault end, and only 3 of these are among the 24. Whether a side is cut off, used alone as a predictor, gives an AUC of 0.36. Dropping every cut-off side removes the 47 ruptures that are cut off on both sides, keeps all 24 that span the fault, and raises the gain to 0.095, with an interval from 0.042 to 0.159. Replacing each cut-off width by the largest width that is not cut off lowers the gain to 0.065, with an interval from 0.017 to 0.123. The gain therefore changes with the rule for a cut-off width. The reported gain uses the rule fixed before the runs, which keeps the last 0.1 km step that remains on the fault.

3.4 Stress amplitude

At a standard deviation of 0.343 times the strength drop, 12 of 42 ruptures span the fault and the gain is 0.125. At 0.393, 8 of 56 span and the gain is 0.049. At 0.443 only 4 of 60 span, too few to compute an AUC. The gain is positive at both levels with enough cases.

3.5 Dynamic overshoot of the static arrest point

Among the 134 ruptures that stop in both calculations, the dynamic tip on the side with the larger subcritical width passed the static arrest point by a median of 0.61 km (Fig. 3b). The median subcritical width on that side is 20.6 km. Their rank correlation is -0.53. In 20 of the 134 the dynamic tip passed the whole subcritical stretch and the rupture still did not span the fault. Passing the static arrest point, crossing the subcritical stretch, and spanning the fault are therefore three different outcomes.

3.6 Distance to the fault end

The width is also longer when the arrest point lies farther from the end of the fault. The subcritical width and the distance from that tip to the end of the fault have a rank correlation of 0.53. In a later calculation, that distance was added to the static arrest length before the width was added. Scoring each rupture with a model fitted without it, the gain from the width is then 0.080, with an interval from 0.030 to 0.155. Adding instead the position of the arrested crack along the fault leaves a gain of 0.083, from 0.034 to 0.147. Neither check was part of the comparison fixed before the new fields were drawn.

4 Discussion

A population model built from static arrests can use the width to choose which arrests to run dynamically, because the width is read from the static crack before any dynamic calculation.
A short subcritical width, read from the static crack, marks a static arrest that is likely to span the fault. The separation comes from 158 ruptures withheld from the fit. The length estimate remains the static rule of Ampuero et al. (2006). The width indicates which of those stops disagree with the dynamic rupture. Two later checks add the distance from the arrest point to the fault end, or the position of the arrested crack. The gain from the width remains 0.080 and 0.083. Both checks were run after the fields had been drawn. On the earlier 52 in-plane ruptures the gain was 0.036 and the interval included zero (Lyu 2026a). Those fields were not drawn again.
The gain above is for one correlation length, 2.03 km. A separate calculation by the author, under review and not yet public, uses stress fields whose measured median correlation length is 1.78 times longer. There a threshold on the width flags 19 of 38 ruptures that span the fault, and a threshold on the static arrest length flags 34 of those 38. The ranking in this letter is the result at 2.03 km.
Weng et al. (2015) set the barrier before the rupture. Galis et al. (2017) multiplied a static area by two after comparing it with three-dimensional dynamic ruptures. The width here is the later extension of a crack the static rule has already stopped. Ripperger et al. (2007) compared dynamic ruptures on random stress with a static estimate. Setting $(1 - \tau_0)$ to 1 in their equation (B15) gives a transition at 0.47. The transition in their Figure 9 lies near 0.3. This paper does not use that equation.
Shear stress on the fault was saved every 1.39 s at 200 m spacing and every 0.69 s at 100 m spacing, and only on the fault. A rupture front at 2 km s^{-1} moves 1 to 3 km between those frames, while the static cohesive-zone estimate Λ is 0.7 km. A brief rise of the dynamic stress intensity factor, a second rupture beyond the subcritical stretch, and the energy balance across that stretch all remain possible. The saved frames cannot separate those three possibilities.

5 Conclusions

On the ruptures tested here, the subcritical width shows which static arrests later span the fault, and the static arrest length alone does not. Two logistic models were fitted on 52 earlier antiplane ruptures and applied unchanged to 158 new ruptures that a static stress-intensity criterion stops. A short subcritical width makes a dynamically spanning rupture more likely. Added to the static arrest length, the width raises the AUC by 0.076, with a 95% interval from 0.037 to 0.126. Halving the grid spacing along strike leaves the outcome of all 158 ruptures unchanged. At this correlation length, the width can rank which static arrests should be checked dynamically first. At a correlation length 1.78 times longer, a width threshold flags fewer spanning ruptures than a length threshold. Where both calculations stop, the dynamic tip still goes a median of 0.61 km past the static arrest point, while the median subcritical width on that side is 20.6 km, so clearing the static arrest point leaves most of that width uncrossed. The comparison covers antiplane rupture on one fault, with one correlation length, three amplitudes of the initial stress, and linear slip weakening. A new in-plane set has not been calculated. The saved records are too coarse to separate the three candidate causes.

Declarations

Availability of data and materials

The datasets generated and analyzed during the current study are available in the Zenodo repository, `https://doi.org/10.5281/zenodo.23602567` (Lyu 2026b). Additional file 1, the table of all 158 ruptures, is in that archive, together with the script that recomputes the scores. The dynamic rupture output files are not included. The solver is the public code cited above.

Competing interests

The author declares that he has no competing interests.

Funding

The author received no funding for this work. No funder had a role in the design of the study, the calculations, the writing of the manuscript, or the decision to submit.

Authors' contributions

WL designed the study, carried out the calculations, and wrote the manuscript.

Authors' information

WL is at the School of Civil Engineering, China University of Mining and Technology, Xuzhou, China. ORCID: 0009-0009-3039-7727.

Acknowledgments

The author used AI-based tools to improve the language and readability. After using these tools, the author reviewed and edited the content and takes full responsibility for it. No AI tool generated the calculations, the numerical results, or the figures.

References

Ampuero JP, Ripperger J, Mai PM (2006) Properties of dynamic earthquake ruptures with heterogeneous stress drop. In: Earthquakes: Radiated Energy and the Physics of Faulting. Geophysical Monograph Series, vol 170. American Geophysical Union, Washington, pp 255-261. doi:10.1029/170GM25

Andrews DJ (1976) Rupture propagation with finite stress in antiplane strain. J Geophys Res 81(20):3575-3582. doi:10.1029/JB081i020p03575

Campillo M, Ionescu IR (1997) Initiation of antiplane shear instability under slip dependent friction. J Geophys Res Solid Earth 102(B9):20363-20371. doi:10.1029/97JB01508

Daub EG (2017) fdfault: a finite-difference code for elastodynamic rupture problems. Version 1.0. https://github.com/edaub/fdfault. Accessed 2 Nov 2026

Day SM, Dalguer LA, Lapusta N, Liu Y (2005) Comparison of finite difference and boundary integral solutions to three-dimensional spontaneous rupture. J Geophys Res Solid Earth 110:B12307. doi:10.1029/2005JB003813

Dunham EM (2007) Conditions governing the occurrence of supershear ruptures under slip-weakening friction. J Geophys Res Solid Earth 112:B07302. doi:10.1029/2006JB004717

Galis M, Ampuero JP, Mai PM, Cappa F (2017) Induced seismicity provides insight into why earthquake ruptures stop. Sci Adv 3(12):eaap7528. doi:10.1126/sciadv.aap7528

Ida Y (1972) Cohesive force across the tip of a longitudinal-shear crack and Griffith's specific surface energy. J Geophys Res 77(20):3796-3805. doi:10.1029/JB077i020p03796

Lyu W (2026a) A static arrest criterion classifies some fault-spanning ruptures as arrested. EarthArXiv preprint. doi:10.31223/X5S51N

Lyu W (2026b) The width beyond a static arrest point predicts which static arrests span the fault. Zenodo. doi:10.5281/zenodo.23602567

McLaskey GC, Kammer DS, Ke C-Y (2026) Earthquake populations from stochastic stress fields. J Geophys Res Solid Earth 131(7):e2025JB033674. doi:10.1029/2025JB033674

Paglialunga F, Ampuero JP, Passelègue F (2026) Stress barriers and their impact on rupture propagation. J Geophys Res Solid Earth 131(2):e2025JB032879. doi:10.1029/2025JB032879

Palmer AC, Rice JR (1973) The growth of slip surfaces in the progressive failure of over-consolidated clay. Proc R Soc Lond A 332(1591):527-548. doi:10.1098/rspa.1973.0040

Ripperger J, Ampuero JP, Mai PM, Giardini D (2007) Earthquake source characteristics from dynamic rupture with constrained stochastic fault stress. J Geophys Res Solid Earth 112:B04311. doi:10.1029/2006JB004515

Uenishi K, Rice JR (2003) Universal nucleation length for slip-weakening rupture instability under nonuniform fault loading. J Geophys Res Solid Earth 108(B1):2042. doi:10.1029/2001JB001681

Weng H, Huang J, Yang H (2015) Barrier-induced supershear ruptures on a slip-weakening fault. Geophys Res Lett 42(12):4824-4832. doi:10.1002/2015GL064281

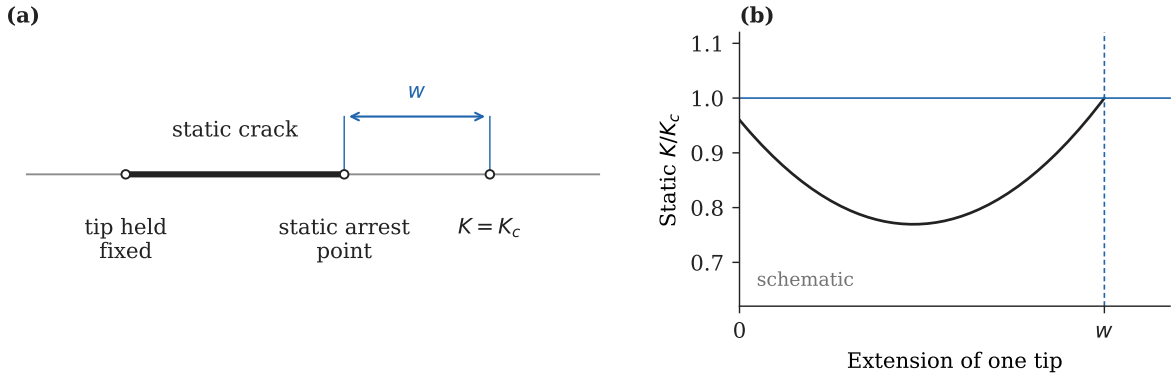


Figure 1. Definition of the subcritical width. (a) One tip of the static crack is held fixed and the other is extended until the static stress intensity factor returns to its critical value. The width w is that extension. (b) A sketch of the return to the critical value.

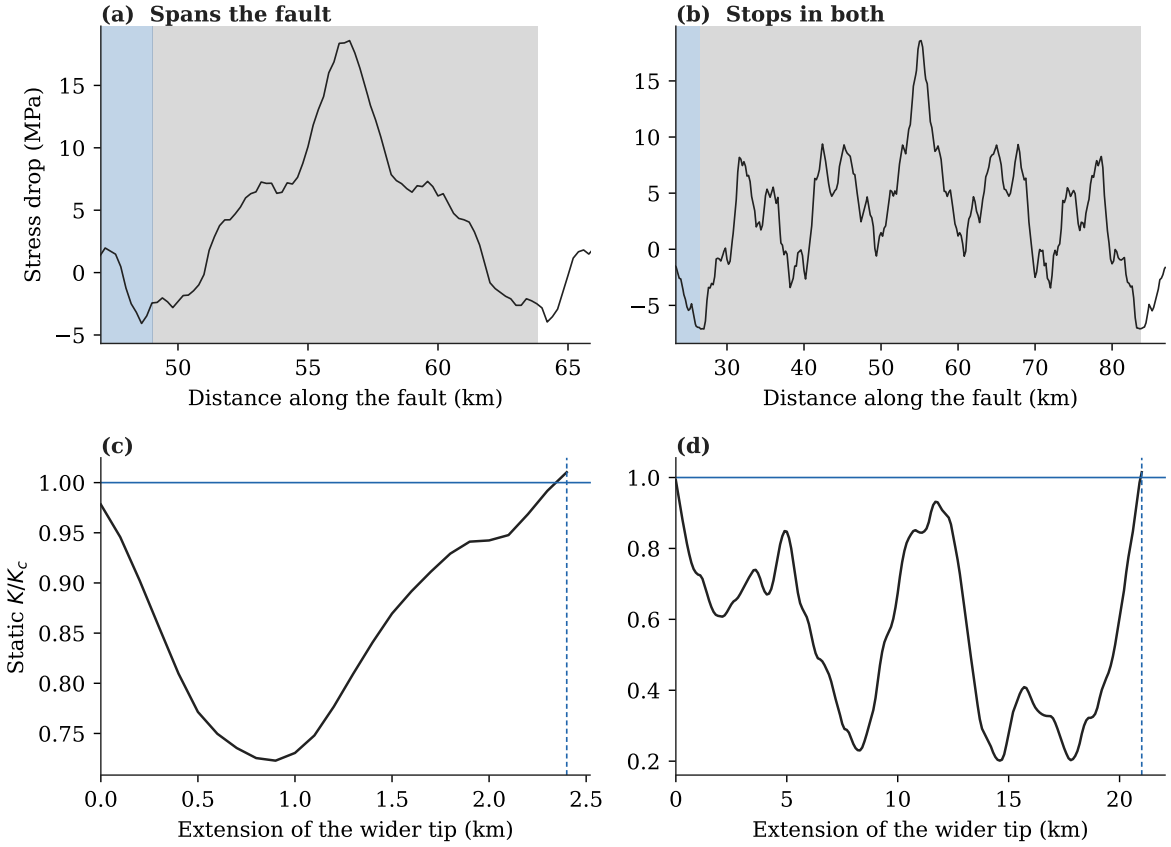


Figure 2. Subcritical width on two ruptures. The left column is near the median width of ruptures that span the fault, and the right column is near the median width of ruptures that stop in both calculations. The upper panels show the initial shear stress minus the residual stress, on the part of the fault around the static crack. The gray band is the static crack and the blue band is the extension of its wider tip, with the other tip held fixed. The lower panels show the static stress intensity factor at that tip, divided by its critical value, against the extension. The dashed line is the recorded width, where the factor returns to the critical value. The horizontal scales of the two ruptures differ.

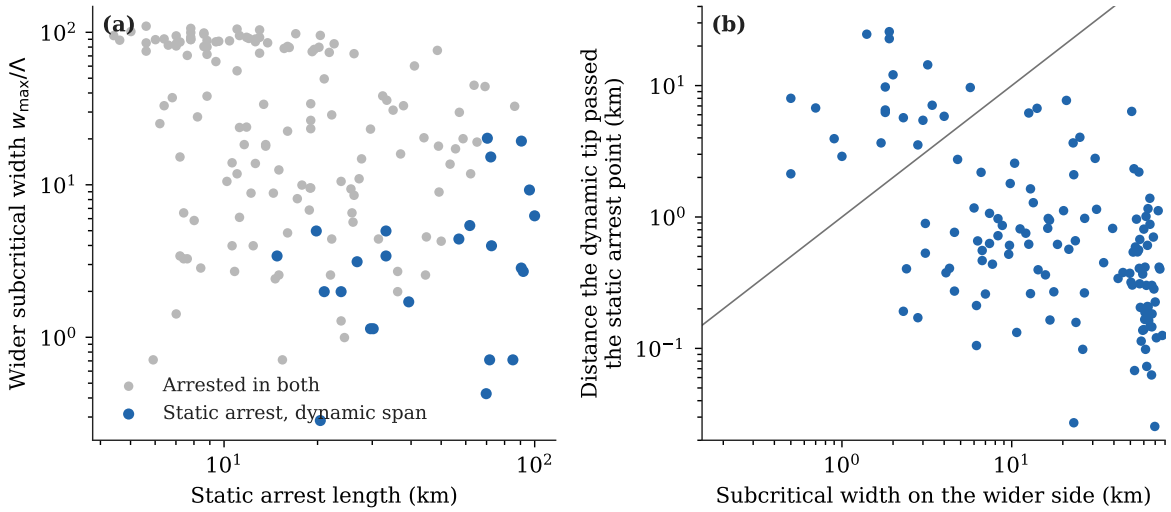


Figure 3. Arrest length and subcritical width. (a) Static arrest length and subcritical width for the 158 ruptures that the static criterion stops. Blue filled symbols span the fault in the dynamic calculation and gray symbols stop in both. The width is the larger of the two sides, divided by $\Lambda = 0.703$ km. (b) For the 134 that also stop dynamically, the distance by which the dynamic tip passed the static arrest point against the subcritical width on the same side, both in kilometers. The line marks equal values.

Additional file 1

Table A1. The 158 ruptures that the static criterion stops. A dash means that tip already lies on an end of the fault, so that side has no width. Cut off means the width stopped at the last 0.1 km step that remains on the fault. Spans means the dynamic rupture reaches at least 108 km.

Stress fraction	Length (km)	Left (km)	Right (km)	Left cut off	Right cut off	Spans 200 m	Spans 100 m
0.343	7.4135	2.300	2.300	no	no	no	no
0.343	72.2135	10.700	6.300	no	yes	yes	yes
0.343	8.4135	2.000	2.000	no	no	no	no
0.343	29.6135	0.800	0.800	no	no	yes	yes
0.343	8.6135	41.700	69.600	yes	yes	no	no
0.343	33.2135	3.500	3.500	no	no	yes	yes
0.343	22.2135	3.100	3.100	no	no	no	no
0.343	71.6135	0.500	0.500	no	no	yes	yes
0.343	61.8135	3.800	3.800	no	no	yes	yes
0.343	7.6135	2.300	2.300	no	no	no	no
0.343	11.2135	16.700	16.700	no	no	no	no
0.343	90.5423	2.000	—	no	—	yes	yes
0.343	49.2135	6.300	6.300	no	no	no	no
0.343	32.4135	26.900	26.900	no	no	no	no
0.343	11.0135	39.300	39.300	no	no	no	no
0.343	19.0135	6.700	6.700	no	no	no	no
0.343	26.2135	42.800	50.900	yes	yes	no	no
0.343	23.8135	7.400	7.400	no	no	no	no
0.343	13.6135	12.900	12.900	no	no	no	no
0.343	91.8949	1.900	—	no	—	yes	yes
0.343	7.8135	63.000	49.100	yes	yes	no	no
0.343	26.8135	2.200	2.100	no	no	yes	yes
0.343	10.2135	7.400	7.400	no	no	no	no
0.343	7.2135	60.700	52.000	yes	yes	no	no
0.343	12.4135	2.800	2.800	no	no	no	no
0.343	14.8135	2.400	2.400	no	no	yes	yes
0.343	69.2135	31.000	7.300	no	yes	no	no
0.343	21.0135	1.400	1.400	no	no	yes	yes
0.343	16.0135	3.400	3.400	no	no	no	no
0.343	26.2135	6.000	6.000	no	no	no	no
0.343	11.8135	16.800	16.800	no	no	no	no
0.343	19.0135	16.400	16.400	no	no	no	no
0.343	20.4135	0.200	0.200	no	no	yes	yes
0.343	7.6135	49.600	39.400	no	yes	no	no
0.343	31.4135	3.100	3.100	no	no	no	no
0.343	53.4135	9.600	9.600	no	no	no	no
0.343	27.2135	7.700	7.700	no	no	no	no
0.343	65.2135	9.900	13.400	yes	no	no	no
0.343	85.0813	—	0.500	—	no	yes	yes
0.343	57.2135	21.000	21.000	no	no	no	no
0.343	33.4135	25.100	25.200	no	no	no	no
0.343	24.4135	0.700	0.600	no	no	no	no
0.393	13.0135	65.100	41.700	yes	yes	no	no
0.393	19.2135	48.200	52.500	yes	yes	no	no
0.393	41.0135	36.600	42.300	yes	yes	no	no
0.393	15.6135	49.200	55.100	yes	yes	no	no
0.393	86.2135	0.700	23.000	yes	no	no	no
0.393	7.0135	57.200	55.700	yes	yes	no	no
0.393	13.0135	51.300	34.800	no	yes	no	no
0.393	36.2135	1.900	1.900	no	no	no	no
0.393	9.4135	44.200	45.200	yes	no	no	no
0.393	18.9135	6.700	6.500	no	no	no	no
0.393	25.8135	4.600	4.600	no	no	no	no
0.393	11.6135	12.900	12.900	no	no	no	no
0.393	6.4135	23.200	23.200	no	no	no	no
0.393	22.0135	1.700	1.800	no	no	no	no
0.393	13.6135	12.600	12.600	no	no	no	no
0.393	99.9542	4.400	—	no	—	yes	yes
0.393	16.2135	55.900	47.800	yes	yes	no	no
0.393	11.8135	65.200	42.900	yes	yes	no	no
0.393	27.7135	10.400	10.300	no	no	no	no
0.393	29.6135	16.300	16.300	no	no	no	no
0.393	12.2135	6.200	6.200	no	no	no	no

Table A1, continued

Stress fraction	Length (km)	Left (km)	Right (km)	Left cut off	Right cut off	Spans 200 m	Spans 100 m
0.393	15.4135	0.500	0.500	no	no	no	no
0.393	14.4135	6.200	6.200	no	no	no	no
0.393	70.4135	14.200	14.200	no	no	yes	yes
0.393	5.9135	0.400	0.500	no	no	no	no
0.393	13.0135	34.000	72.900	yes	yes	no	no
0.393	33.2135	2.400	2.400	no	no	yes	yes
0.393	37.0135	11.200	11.200	no	no	no	no
0.393	39.3135	1.200	1.100	no	no	yes	yes
0.393	44.0135	14.300	14.300	no	no	no	no
0.393	9.6135	61.400	48.800	yes	yes	no	no
0.393	5.6135	52.900	46.700	no	yes	no	no
0.393	62.2135	8.300	8.300	no	no	no	no
0.393	20.2135	56.100	43.500	yes	yes	no	no
0.393	12.6135	63.500	43.800	yes	yes	no	no
0.393	7.0135	66.600	46.300	yes	yes	no	no
0.393	15.0135	1.800	1.800	no	no	no	no
0.393	23.8135	1.400	1.400	no	no	yes	yes
0.393	8.0135	4.100	4.100	no	no	no	no
0.393	19.0135	18.600	18.600	no	no	no	no
0.393	14.6135	1.700	1.700	no	no	no	no
0.393	8.8135	56.400	54.700	yes	yes	no	no
0.393	21.0135	34.800	34.800	no	no	no	no
0.393	17.2135	5.700	5.700	no	no	no	no
0.393	6.0135	62.900	50.900	yes	yes	no	no
0.393	19.8135	3.500	3.500	no	no	yes	yes
0.393	13.4135	23.700	23.700	no	no	no	no
0.393	15.0135	8.800	8.800	no	no	no	no
0.393	96.2135	0.600	6.500	yes	no	yes	yes
0.393	22.2135	20.200	20.200	no	no	no	no
0.393	7.0135	1.000	1.000	no	no	no	no
0.393	57.0135	3.100	3.100	no	no	yes	yes
0.393	7.4135	4.600	4.600	no	no	no	no
0.393	7.2135	10.700	10.700	no	no	no	no
0.393	13.8135	46.100	60.000	yes	yes	no	no
0.393	25.6135	6.600	6.600	no	no	no	no
0.443	7.0135	59.100	53.800	yes	yes	no	no
0.443	5.6135	77.100	37.200	yes	yes	no	no
0.443	20.4135	67.100	32.400	yes	yes	no	no
0.443	11.2135	66.900	41.800	yes	yes	no	no
0.443	5.6135	54.400	59.900	yes	yes	no	no
0.443	7.8135	65.300	46.800	yes	yes	no	no
0.443	16.0135	15.800	15.800	no	no	no	no
0.443	12.0135	64.100	43.800	yes	yes	no	no
0.443	9.4135	60.900	49.500	yes	yes	no	no
0.443	11.0135	8.300	8.300	no	no	no	no
0.443	44.5135	1.800	1.700	no	no	no	no
0.443	90.6135	10.900	13.600	yes	no	yes	yes
0.443	48.6135	17.700	53.500	yes	yes	no	no
0.443	16.0135	56.800	47.100	yes	yes	no	no
0.443	4.4135	48.600	66.900	yes	yes	no	no
0.443	7.8135	74.600	37.500	yes	yes	no	no
0.443	30.2135	0.700	0.800	no	no	yes	yes
0.443	12.6135	61.000	46.300	yes	yes	no	no
0.443	12.6135	9.700	9.700	no	no	no	no
0.443	10.8135	1.900	1.900	no	no	no	no
0.443	8.6135	43.000	68.300	yes	yes	no	no
0.443	36.2135	1.400	1.400	no	no	no	no
0.443	10.4135	61.800	47.700	yes	yes	no	no
0.443	8.8135	49.000	62.100	yes	yes	no	no
0.443	55.6135	12.100	12.100	no	no	no	no
0.443	6.4135	49.900	63.600	yes	yes	no	no
0.443	8.2135	19.600	19.600	no	no	no	no
0.443	10.6135	2.800	2.800	no	no	no	no
0.443	26.0135	4.000	4.000	no	no	no	no
0.443	35.0135	21.700	21.700	no	no	no	no
0.443	8.8135	26.800	26.800	no	no	no	no
0.443	7.8135	49.100	63.000	yes	yes	no	no
0.443	11.0135	73.800	35.100	yes	yes	no	no
0.443	11.2135	4.200	4.300	no	no	no	no
0.443	6.2135	17.700	17.700	no	no	no	no
0.443	72.6135	2.800	2.800	no	no	yes	yes

Table A1, continued

Stress fraction	Length (km)	Left (km)	Right (km)	Left cut off	Right cut off	Spans 200 m	Spans 100 m
0.443	6.6135	57.900	55.400	yes	yes	no	no
0.443	69.8135	0.300	0.300	no	no	yes	yes
0.443	10.6135	9.700	9.800	no	no	no	no
0.443	8.6135	56.700	54.600	yes	yes	no	no
0.443	63.8135	31.600	13.000	no	yes	no	no
0.443	5.0135	43.800	71.100	yes	yes	no	no
0.443	8.8135	50.400	50.400	no	no	no	no
0.443	50.0135	3.000	3.000	no	no	no	no
0.443	58.8135	14.100	14.100	no	no	no	no
0.443	4.6135	52.900	62.400	yes	yes	no	no
0.443	19.0135	23.900	23.900	no	no	no	no
0.443	7.8135	70.000	42.100	yes	yes	no	no
0.443	21.8135	46.200	51.900	yes	yes	no	no
0.443	18.8135	4.800	4.800	no	no	no	no
0.443	17.0135	68.800	34.100	yes	yes	no	no
0.443	22.6135	38.200	59.100	yes	yes	no	no
0.443	49.0135	12.600	12.600	no	no	no	no
0.443	6.8135	26.200	26.200	no	no	no	no
0.443	7.2135	2.400	2.400	no	no	no	no
0.443	44.8135	3.200	3.200	no	no	no	no
0.443	19.5135	54.300	46.100	yes	yes	no	no
0.443	37.8135	23.200	23.200	no	no	no	no
0.443	23.8135	0.900	0.900	no	no	no	no
0.443	17.8135	7.000	7.000	no	no	no	no